ACS APPLIED MATERIALS & INTERFACES

Research Article

www.acsami.org

Adsorption Behaviors of DNA/Cation Complexes on Amino and Silica Chip Surfaces: A Dual Polarization Interferometry Study

Fujian Huang[†] and Haojun Liang*[,†,‡]

[†]CAS Key Laboratory of Soft Matter Chemistry, Collaborative Innovation Center of Chemistry for Energy Materials, Department of Polymer Science and Engineering, University of Science and Technology of China, Hefei, Anhui 230026, People's Republic of China

[‡]Hefei National Laboratory for Physical Sciences at Microscale, University of Science and Technology of China, Hefei, Anhui 230026, People's Republic of China

Supporting Information

ABSTRACT: The adsorption of DNA/Ca^{2+}, DNA/Cu^{2+}, and DNA/$Co(NH_3)_6^{3+}$ complexes on amino and silica chip surfaces were investigated using dual polarization interferometry. A more compact DNA/cation complex layer formed on the amino chip surface compared with that on the silica chip surface at the same cation condition. The real-time mass, thickness, and density changes were monitored during the adsorption process. The overall results show that the approaching complexes can cause the conformation rearrangement of the preadsorbed complexes and the preadsorbed complexes affect the deposition pattern of the approaching complexes during the adsorption of DNA/Ca^{2+} and DNA/Cu^{2+} complexes on both chip surfaces. The relatively strong electrostatic repulsion between the approaching and adsorbed complexes results in multiple mass loading rate changes and loose attachment of the approaching complexes. The weak repulsion between the DNA/$Co(NH_3)_6^{3+}$ complexes cannot induce this kind of conformation rearrangement. Thus, no multiple mass loading rate changes were observed. Meanwhile, the preadsorbed DNA/$Co(NH_3)_6^{3+}$ complex can also affect the deposition pattern of the approaching complex because of the geometric resistance. Therefore, this study will help better understand the conformation change and deposition pattern of complexes with different charge conditions during the adsorption process on the solid–liquid interface.

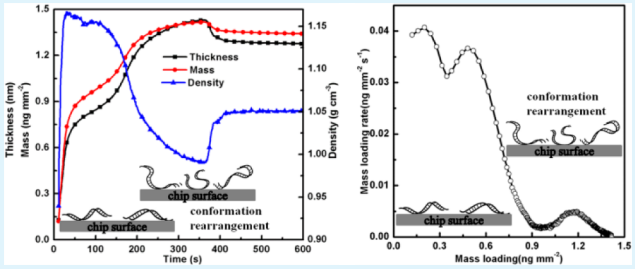

KEYWORDS: *DNA/cation complexes, zeta potential, solid–liquid interface, adsorption dynamics, conformation rearrangement, dual polarization interferometry*

1. INTRODUCTION

DNA adsorption on a solid surface is important in various fields, such as in DNA-based biosensing,[1−4] DNA microarrays,[5,6] DNA hybridization studies,[7−9] a small molecule–DNA interaction study,[10] mesoporous silica nanoparticle-based gene delivery,[11−14] and DNA separation and purification through solid-phase extraction.[15,16] Double-stranded DNA is a highly negatively charged biomacromolecule.[17] Thus, studying DNA adsorption on a surface will help determine the adsorption process of highly negatively charged polyelectrolytes on the liquid–solid interface.

Double-stranded DNA can interact with cation, forming a DNA/cation complex. Different cations cause different interactions with the bases and phosphate groups of DNA.[18−23] Raman spectroscopy[24] has proven that DNA has stronger interaction with Cu^{2+} compared with Ca^{2+}. $Co(NH_3)_6^{3+}$ can interact with DNA through major groove binding and electrostatic interaction with the DNA phosphate groups, making the DNA condense.[23,25−29] In the past two decades, several studies have investigated the interaction between DNA and cations as well as the charge and conformation of DNA/cation complexes in solution. However, the adsorption process, especially the adsorption dynamics and conformation information of these complexes during the adsorption process on the solid–liquid interface, is not yet clearly understood. DNA can interact with cations, forming DNA/cation complexes with different charge and conformation conditions. Studying the adsorption of these complexes on different surfaces can help us better understand how the charge condition of complex, complex–surface interaction, and surface charge condition affect the adsorption behavior and conformation change of DNA/cation complex adsorbed on the solid–liquid interface.

To date, atomic force microscopy (AFM),[30−32] quartz crystal microbalance with dissipation monitoring (QCM-D),[33−39] surface plasmon resonance (SPR),[40−42] and ellipsometry[43−47] have been widely used to study the polyelectrolyte adsorption kinetics and conformation of adsorbed polyelectrolyte on the surface. In most cases, the time scales of some of the kinetic steps overlap, making them difficult to separate during experiments.[48] This issue challenges one from accurately describing and distinguishing the kinetic steps when using the

Received: March 5, 2013
Accepted: May 22, 2013
Published: May 22, 2013

   dx.doi.org/10.1021/am400813x | ACS Appl. Mater. Interfaces 2013, 5, 5025−5033

above techniques to study the adsorption of macromolecules at the solid−liquid interface.

Dual polarization interferometry (DPI) is a surface-sensitive technique used in the solid−liquid interface for the simultaneous real-time, time-efficient, label-free, and quantitative measurement of changes in layer mass, thickness, and density. DPI provides real-time information of the adsorbed species and elucidates the layer by layer assembly mechanism of oppositely charged polymers.[49] It has also been applied to various study areas including protein structure changes, polyelectrolyte assemblies, oligonucleotide hybridization, and biomimic biomembranes.[50−53] These studies show the potential of DPI for studying the adsorption behavior and conformation information of the DNA/cation complex during the adsorption on the solid−liquid interface.

In current study, three types of DNA/cation complexes with different charges were prepared by dissolving DNA in 1 mM $CaCl_2$, $CuSO_4$, and $Co(NH_3)_6Cl_3$ aqueous solution. The zeta potentials and electrophoretic mobilities were measured using a Zetasizer Nano ZS instrument. The real-time mass, thickness, and density changes during the adsorption on amino and silica chip surfaces were recorded using DPI. On the basis of the real-time parameters, the adsorption behaviors and conformation changes during adsorption were investigated.

2. EXPERIMENTAL SECTION

2.1. Materials and Sample Preparation. The low molecular weight DNA extracted from salmon sperm was purchased from Sigma Chemical Co. Hexammine cobalt(III) chloride and (3-aminopropyl)-trimethoxysilane were obtained from Sangon Biotech Co., Ltd. (Shanghai) and Alfa Co. Calcium chloride, copper sulfate, and other chemicals used were of analytical grade. The water used in the experiments was of Milli-Q grade (Millipore) and degassed before the DPI experiments. The 1 mM solution of $CaCl_2$, $CuSO_4$, and $Co(NH_3)_6Cl_3$ was prepared using Milli-Q water. The DNA aqueous solutions were prepared at 200 μg mL^{-1} using the salt solutions and incubated overnight.

2.2. Collector Surfaces. Silica and amino chips were used during the DPI experiments. The bare sensor chip, FB 80 Unmodified (Farfield Sensors), was first cleaned with 2% (w/v) Hellmanex solution (Hellma GmbH & Co.) for 30 min and then incubated in a hot piranha solution (H_2O_2/H_2SO_4, 3:7,v/v) for 30 min. (*CAUTION*: "Piranha" solution reacts violently with organic materials; it must be handled with extreme care.) Afterward, the chip was fully rinsed with ultrapure water and blown dry with N_2. The chip surface is composed of hydrophilic and negatively charged Si−OH. The amino chip was obtained by silanizing the silica chip. The cleaned silica chip was silanized with a 4% (V/V) solution of (3-aminopropyl)-trimethoxysilane in isopropanol at room temperature for 2 h. The sensor chip was fully rinsed with isopropanol, blown dry with N_2, and then baked at 120 °C for 30 min. This aminated chip surface is slightly hydrophobic with strong positive charge.

2.3. Electrophoretic Mobility Measurements. The zeta potential and electrophoretic mobility of DNA/cation complexes were measured using a Zetasizer Nano ZS instrument to conduct laser Doppler velocimetry (LDV); the instrument has a measurement range spanning from 3 nm to 10 μm. In this technique, a voltage is applied across a pair of electrodes that are placed at both ends of a cell that contains particle dispersion. Charged particles are attracted to the oppositely charged electrode, and their velocity is measured and expressed per unit field strength as the electrophoretic mobility, μe.

2.4. Dual Polarization Interferometry Experiments. The DNA/cation complex adsorptions on amino and silica chip surfaces were evaluated in real time using DPI (AnaLight Bio200, Farfield Group Ltd., Crewe, UK). The details of the technique and theory were described previously.[51,52] The instrument uses a helium−neon laser emitting light at 632.8 nm, which measures the optical phase changes in an evanescent dual polarization interferometer. The polarization state of the light is switched between transverse-electric (T_E) and transverse-magnetic (T_M) via a polarizer. The fluidic system coupled with the instrument consists of a high-performance liquid chromatography injector valve and an external pump (Harvard Apparatus, PHD2000) that provides a controlled continuous fluid flow over two channels on the chip surface. All DPI experiments were performed at 20 ± 0.002 °C using pure water as running buffer. Before each experiment, the sensor chip was calibrated using an 80% (w/w) ethanol/water solution and ultrapure water, of which the refractive indexes (RIs) are known to calibrate the waveguide thickness and RI. The data were analyzed using an AnaLight Bio200 instrument for subsequent calculations.

After calibration, the flow rate was changed to 25 μL min^{-1}. Before the injection of DNA/cation complex, a cation solution was injected to ensure the surface was saturated with cations. The DNA/cation complex solutions were then injected independently into the chip surface for 6 min and then rinsed with Milli-Q water. The phase changes of T_E and T_M were recorded in real time. The absolute layer thickness and RI were resolved directly from the T_M and T_E phase values using analysis software. The adsorbed mass was quantified according to the De Feijter's equations as follows:[54]

$$\rho_L = \frac{n_L - n_{buffer}}{dn/dc} \quad (1)$$

$$m_L = \rho_L \cdot \tau_L \quad (2)$$

where m_L is the layer mass per unit area (ng mm^{-2}), τ_L is the layer thickness (nm), n_L and n_{buffer} are the RIs of the adsorbed layer and the bulk solution, respectively, and dn/dc is the RI increment (cm^3 g^{-1}) of the DNA. A dn/dc value of 0.183 was used according to Tumolo et al.[55]

According to the above-mentioned calculated parameters, the adsorption mechanism of DNA/cation complexes on amino and silica chip surfaces can be inferred. The parameters were recorded real time so that the adsorption dynamics can also be evaluated.

3. RESULTS AND DISCUSSION

3.1. Formation and Properties of DNA/Cation Complexes. Double-stranded DNA is a highly negatively charged biopolymer with a persistence length of about 50 nm.[17] In addition to being a biologic carrier of genetic information, DNA in the solution exhibits unusual polyelectrolyte behaviors. The addition of multivalent salts into the DNA solution can form a homogeneous solution or result in the phase separation.[56−58]

In our study, we prepared DNA/cation complexes by dissolving DNA at a concentration of 200 μg mL^{-1} in three different salt solutions and incubating overnight. All salt concentrations were 1 mM. The measured zeta potentials of DNA/Ca^{2+}, DNA/Cu^{2+}, and DNA/$Co(NH_3)_6^{3+}$ complexes were −33.3, −22.4, and −4.09 mV, respectively, and the corresponding electrophoretic mobilities were -2.61×10^{-8}, -1.759×10^{-8}, and -0.3206×10^{-8} m^2 (V·s)$^{-1}$, indicating that the negative charges of DNA/cation complexes decrease as follows: DNA/Ca^{2+} > DNA/Cu^{2+} > DNA/$Co(NH_3)_6^{3+}$. According to Duguid et al.,[24] Cu^{2+} strongly interacts with DNA phosphate groups and bases, whereas Ca^{2+} weakly interacts with both bases and phosphate groups. Cations adsorbed on the DNA chain can neutralize the DNA negative charges, reducing the intersegmental repulsion and making the DNA chain coiled. In our study, DNA adsorbed more Cu^{2+} compared with Ca^{2+}, making the DNA/Cu^{2+} complex less negatively charged compared with the DNA/Ca^{2+} complex at the same cation concentration.

$Co(NH_3)_6^{3+}$ interacts with DNA through major groove binding and electrostatic interaction with the DNA phosphate

groups, making DNA condense.[28] The DNA/$Co(NH_3)_6^{3+}$ complex is the least negatively charged complex among the three studied complexes because trivalent $Co(NH_3)_6^{3+}$ can most effectively neutralize the negative charge compared to the other two cations. Thus, the repulsion between the $Co(NH_3)_6^{3+}$ complexes is not as dramatic as that of the DNA/Cu^{2+} and DNA/Ca^{2+} complexes.

3.2. Adsorbed Layer Parameters. Three different DNA/cation complex solutions were injected independently into the amino and silica chip surfaces for 6 min. The valve was then switched, and the surfaces were contacted with pure water. During rinsing, several loosely attached complexes were washed away until a stable state was reached. The adsorbed layer parameters were then resolved directly from the stable T_E and T_M phase values using analysis software. The key parameters for the adsorbed layers are listed in Table 1, wherein the loading

Table 1. Key Parameters Obtained from DPI Analysis of the Adsorbed Layers

DNA/cation complex	surface condition	thickness (nm)	mass (ng mm^{-2})	density (g cm^{-3})
DNA/Ca^{2+}	silica chip	0.709	0.2296	0.29
DNA/Cu^{2+}	silica chip	2.1377	0.78	0.3656
DNA/$Co(NH_3)_6^{3+}$	silica chip	2.6498	1.57	0.5925
DNA/Ca^{2+}	amino chip	1.2718	1.3388	1.0526
DNA/Cu^{2+}	amino chip	1.9924	1.7361	0.8714
DNA/$Co(NH_3)_6^{3+}$	amino chip	4.1056	3.7329	0.909

mass and adsorbed layer thickness of the DNA/cation complexes on both amino and silica chip surfaces increase as follows: DNA/$Co(NH_3)_6^{3+}$ > DNA/Cu^{2+} > DNA/Ca^{2+}. The most compact layer (highest density) was obtained in the DNA/Ca^{2+} complex adsorption on the amino chip surface, and the most thick layer was obtained in the DNA/$Co(NH_3)_6^{3+}$ complex adsorption on amino chip surface.

The silica chip surface is composed of Si−OH. Under the tested solution conditions, both the silica surface[59] and DNA are negatively charged, resulting in electrostatic repulsion. Therefore, pure DNA cannot be adsorbed on the silica surface without the help of cations. In the solutions containing Ca^{2+}, Cu^{2+}, and $Co(NH_3)_6^{3+}$, the silanols on silica surface adsorb or react with these cations, forming the $SiOM^+$ complex surface, where M represents a metal. Moreover, these cations can also interact with the DNA chain, introducing some positive charge in the chain. These interactions reduce the overall negative charge of the silica surface and DNA chain, promoting the adsorption of polynucleotides. According to Stumm et al.,[60] $Co(NH_3)_6^{3+}$ and Cu^{2+} have higher association constants to the silica surface compared with Ca^{2+}, which means that the silica surface is more negatively charged in Ca^{2+} solution compared with that in Cu^{2+} and $Co(NH_3)_6^{3+}$ solutions. In addition, the negative charges of DNA/Cu^{2+} and DNA/$Co(NH_3)_6^{3+}$ complexes are much lower than that of the DNA/Ca^{2+} complex. The combination of these two factors leads to a high mass loading of DNA/Cu^{2+} and DNA/$Co(NH_3)_6^{3+}$ complexes on the silica chip surface.

For the adsorptions on the amino chip surface, the chip surface is composed of positively charged Si−$(CH_2)_3$−NH_2 under the tested solution conditions.[59,61] DNA/cation complexes were adsorbed on the amino chip surface via electrostatic interactions, hydrogen binding interactions, and Van der Waal's force. Under the same cation environment, more DNA/cation complexes were adsorbed on the amino chip surface compared with that on the silica chip surface. If we plot the thickness change against mass loading (see Figure S2 in the Supporting Information), all the curves obtained in the adsorptions on the amino chip surface are under that of the silica chip surface, indicating that DNA/cation complexes were adsorbed more compactly on the amino chip surface than that on the silica chip surface.

The DNA/Ca^{2+} complex is the most negatively charged and extended, compared to the other two DNA/cation complexes. This extended DNA/Ca^{2+} was adsorbed on the amino chip surface most flatly and compactly, forming a highly dense layer. The repulsion between the DNA/Ca^{2+} complexes is dramatic, and the negative charge on the complex can effectively counteract the positive charge on the amino chip surface. Although the interaction between DNA/Ca^{2+} and the amino chip is strong, the DNA/Ca^{2+} complex was not continuously adsorbed on the surface because of the dramatic repulsion between DNA/Ca^{2+} complexes, resulting in a relatively low mass loading in the DNA/Ca^{2+} complex adsorption on the amino chip surface. The negative charge of the DNA/Cu^{2+} complex is lower than that of the DNA/Ca^{2+} complex. This complex formed a less flat layer (a higher thickness and lower density compared with the adsorbed DNA/Ca^{2+} complex layer on the amino chip surface) on the amino chip surface. The repulsion between the DNA/Cu^{2+} complexes is not as dramatic as that of the DNA/Ca^{2+} complexes; thus, more DNA/Cu^{2+} complex can be adsorbed on the chip surface (a higher mass loading).

The zeta potential of the DNA/$Co(NH_3)_6^{3+}$ complex is −4.09 mV which is much lower than that of DNA/Ca^{2+} and DNA/Cu^{2+} complexes, indicating that there is almost no repulsion between DNA/$Co(NH_3)_6^{3+}$ complexes. DNA/$Co(NH_3)_6^{3+}$ complex was adsorbed on the amino chip surface via hydrogen binding interaction, Van der Waal's force, and weak electrostatic interaction. These forces are strong enough to make the DNA/$Co(NH_3)_6^{3+}$ complex be adsorbed on the surface. Meanwhile, there is almost no repulsion between the DNA/$Co(NH_3)_6^{3+}$ complexes, and the molecular weight of the DNA/$Co(NH_3)_6^{3+}$ complex is higher compared with the other two complexes. All these factors result in the large adsorption amount of DNA/$Co(NH_3)_6^{3+}$ on the amino chip surface.

3.3. Conformation Changes and Adsorption Dynamics during the Adsorption of DNA/Cation Complexes on Amino Chip Surface. The DNA/cation complexes were adsorbed on the chip surface. Thus, the surface condition changed from bare to full covering, and the condition of the adsorbed complexes on the surface changed from sparse to crowded. This crowded condition will change the layer structure and adsorption behaviors of subsequent complexes if repulsion exists between the DNA/cation complexes. The evolution of the adsorbed layer mass, thickness, and density as a function of time during the adsorption of DNA/cation complexes on the amino chip surface and the adsorption dynamics are investigated in this section.

Figure 1 shows the real-time thickness, mass, and density changes during the adsorption of DNA/Ca^{2+} complex on the amino chip surface. The thickness, mass, and density initially increased rapidly because of the strong electrostatic interaction between the DNA/Ca^{2+} complex and the amino chip surface. With continuous adsorption, the mass and thickness increased less rapidly for about 100 s until a layer mass value of about 1.1 ng mm^{-2} was reached. The layer mass and thickness then

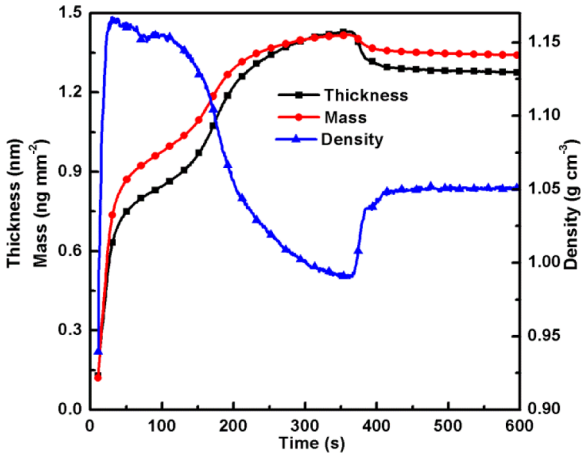

Figure 1. Real-time DPI measurements of thickness, mass, and density during the adsorption of the DNA/Ca^{2+} complex on the amino chip surface.

increased more rapidly again, whereas the layer density decreased dramatically, indicating a different adsorption process happened.

Mass loading rate dm_L/dt was plotted against mass loading m_L to better understand the whole adsorption process (Figure 2). The mass loading rate increased three times. At the

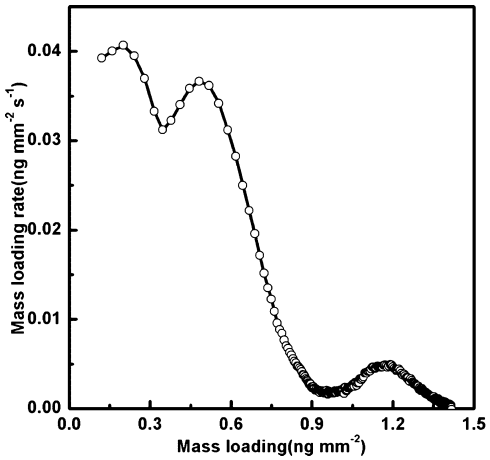

Figure 2. Changes in the mass loading rate as a function of the mass loading of the DNA/Ca^{2+} complex on the amino chip surface during the initial stage of adsorption from Figure 1.

beginning of the adsorption, the mass loading rate increased to a maximum. This first time increase is attributed to the concentration increase of the DNA/Ca^{2+} complex solution over the chip surface. Before the injection of the DNA/Ca^{2+} complex solution, the microfluidic flow chamber was full of pure water. When the DNA/Ca^{2+} solution reached the chamber, it took a few seconds to introduce the solution over the entire chip surface. Thus, the concentration over the chip surface changed from 0 to the maximum and then was kept stable in the following adsorption process. This concentration increase caused the first increase of mass loading rate. With continuous adsorption, more complex occupied the surface, and so, the mass loading rate decreased. Interestingly, a second increase of mass loading rate was observed when the mass loading reached about 0.4 ng mm^{-2}. This phenomenom can be understood from the adsorption process. At the beginning of the adsorption, the chip surface was bare. Thus, the complexes deposited remotely onto the surface, with no repellent among each other. The continuous adsorption changed the state of the adsorbed complexes on the chip surface from sparse to crowded. The adsorbed complexes were so close when the mass loading reached about 0.4 ng mm^{-2} that they began to repel each other. Therefore, to reduce this kind of repulsion and obtain more DNA/Ca^{2+} complex from the solution, the preadsorbed DNA/Ca^{2+} complexes rearranged themselves to make the surface more available for subsequent adsorption, resulting in increased mass loading rate. When the mass loading reached about 1.1 ng mm^{-2}, the mass loading rate increased for the third time, indicating that a second adsorbed layer conformation rearrangement occurred. In contrast, the following adsorption was accompanied with the rapid decrease of adsorbed layer average density, indicating that the subsequent complex attached on the surface loosely.

Two different slopes were observed after we plotted the layer thickness change against the mass loading (Figure 3). The

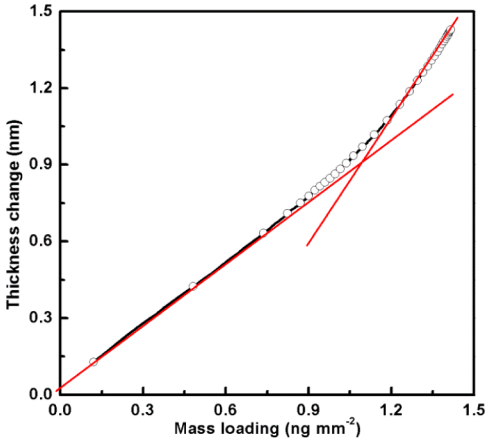

Figure 3. Changes in the layer thickness as a function of the mass loading of the DNA/Ca^{2+} complex on the amino chip surface during the initial stage of adsorption.

result indicates an initial flat conformation followed by a steep increase in layer thickness. The DNA/Ca^{2+} complex was first adsorbed on the amino chip surface as a homogeneous compact layer. A heterogeneous layer may have formed as more complex diffused to the interface. At the break in the slope (1.1 ng mm^{-2}), although the adsorbed complexes rearranged themselves to take more complexes from the solution, the chip surface was so crowded that the following DNA/Ca^{2+} complex could only attach partly onto the surface, resulting in the steep increase in layer thickness and dramatic decrease in layer density.

The adsorption of the DNA/Cu^{2+} complex on the amino chip surface is different from that of the DNA/Ca^{2+} complex because of their different charge conditions and interaction strengths with the amino chip surface. The real-time thickness, mass, and density changes are shown in Figure 4a, wherein the mass and thickness increased rapidly simultaneously at the beginning of the adsorption. When the adsorption amount reached 7.4 ng mm^{-2}, the mass and thickness dramatically decreased rapidly. During the adsorption, the mass loading rate (Figure 5a) also increased three times, similar to the adsorption of the DNA/Ca^{2+} complexes on the amino chip surface. In contrast, the DNA/Cu^{2+} complex can be adsorbed more easily

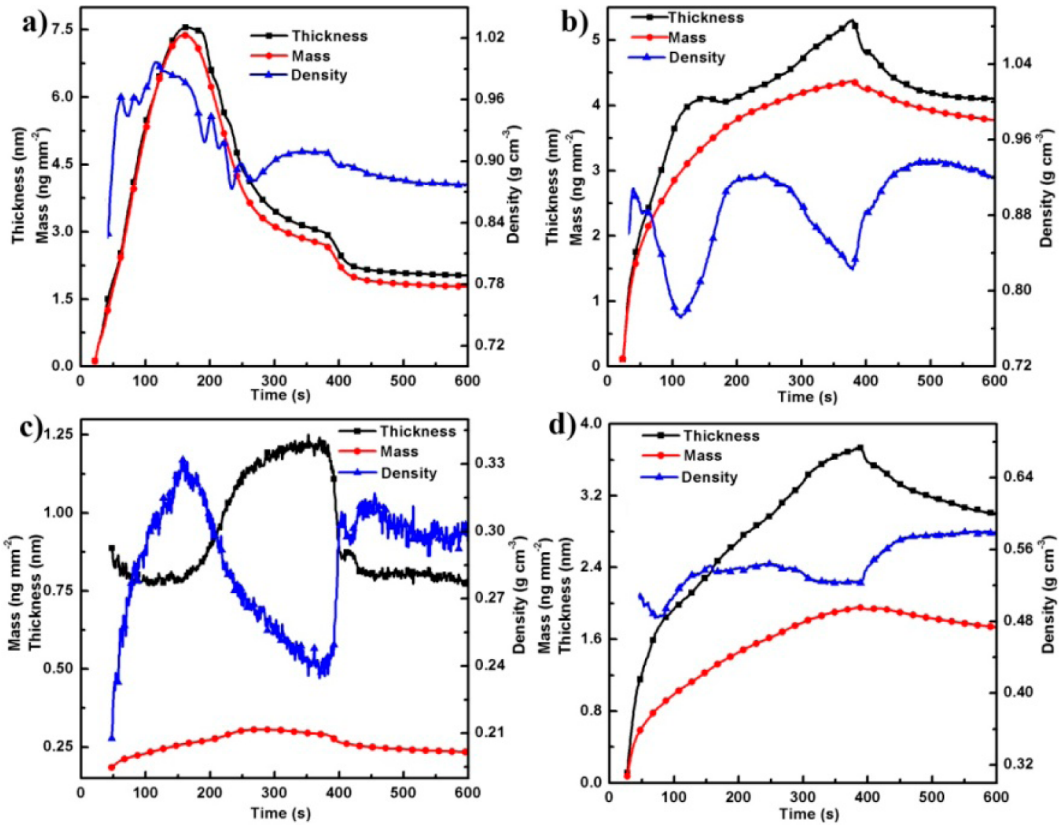

Figure 4. Real-time DPI measurements of thickness, mass, and density during the adsorption of (a) DNA/Cu^{2+} and (b) DNA/$Co(NH_3)_6^{3+}$ complexes on the amino chip surface as well as (c) DNA/Ca^{2+} and (d) DNA/$Co(NH_3)_6^{3+}$ complexes on the silica chip surface.

and continuously on the amino chip surface because of the relatively weak repulsion between complexes. A huge amount of the DNA/Cu^{2+} complexes rapidly deposited onto the amino chip surface, and the adsorbed complexes were in the metastable state. The chip surface was crowded when the mass loading reached 7.4 ng mm^{-2}; thus, most of the preadsorbed complexes were excluded from the surface to keep the remaining adsorbed complexes comfortable and stable, decreasing the mass and thickness.

For the adsorption of the DNA/$Co(NH_3)_6^{3+}$ complex on the amino chip surface, multiple variations of layer thickness and density changes were observed (Figure 4b). At the beginning of the adsorption, the layer thickness, mass, and density increased simultaneously. The layer density began to decrease when the mass loading was 1.8 ng mm^{-2}. Moreover, from the thickness change−mass loading curve (Figure S2 in the Supporting Information, pink curve), we can observe that the curve began to deviate upward from the initial line at this point (1.8 ng mm^{-2}). This upward deviation and density decrease indicate that the same mass loading results in a higher thickness increase compared with the initial adsorption step. Similar to the adsorption of the DNA/Ca^{2+} complex on the amino chip surface, the surface became crowded with the continuous adsorption; thus, the subsequent DNA/$Co(NH_3)_6^{3+}$ complex loosely attached on the surface, decreasing the layer density. In contrast, we cannot observe the multiple mass loading rate increases from the mass loading rate curve (Figure 5b). This means that the crowded surface can just affect the deposition pattern of the following complex, but the approaching complex cannot make the preadsorbed complex rearrange the conformation because of the relatively weak intermolecular electrostatic repulsion between DNA/$Co(NH_3)_6^{3+}$ complexes. In the subsequent adsorption step, the layer density increased and the adsorbed mass marginally increased. Thus, during this adsorption step, the loosely attached complexes relaxed to a more compact structure to allow the negatively charged groups to accommodate to the positively charged surface. The layer density then decreased again, and the layer thickness increased more rapidly. These changes in layer thickness and density with adsorption time demonstrate that some complexes loosely attached again on the almost fully covered surface. After rinsing, the loosely attached complexes can be easily washed off, and so, the layer thickness decreased and the layer density increased to their initial values, indicating that the loosely attached complexes were totally washed off.

3.4. Changes in Layer Morphology and Adsorption Dynamics during the Adsorption of DNA/Cation Complexes on the Silica Chip Surface. The adsorption of polyelectrolytes from an aqueous solution on solid surfaces is strongly dependent on the surface properties, especially the surface charge conditions that affect the polyelectrolytes−surface interactions.[62] The silica chip surface has a quite different surface charge condition compared with the amino chip surface. Thus, the interaction between the DNA/cation complex and the silica chip surface under the same cation condition should be different with the DNA/cation complex−amino chip surface interaction. In this section, the adsorption behaviors of DNA/cation complexes on the silica chip surface have been investigated to understand the effect of surface charge condition on the layer morphology changes and deposition dynamics during the adsorption processes.

dx.doi.org/10.1021/am400813x | ACS Appl. Mater. Interfaces 2013, 5, 5025−5033

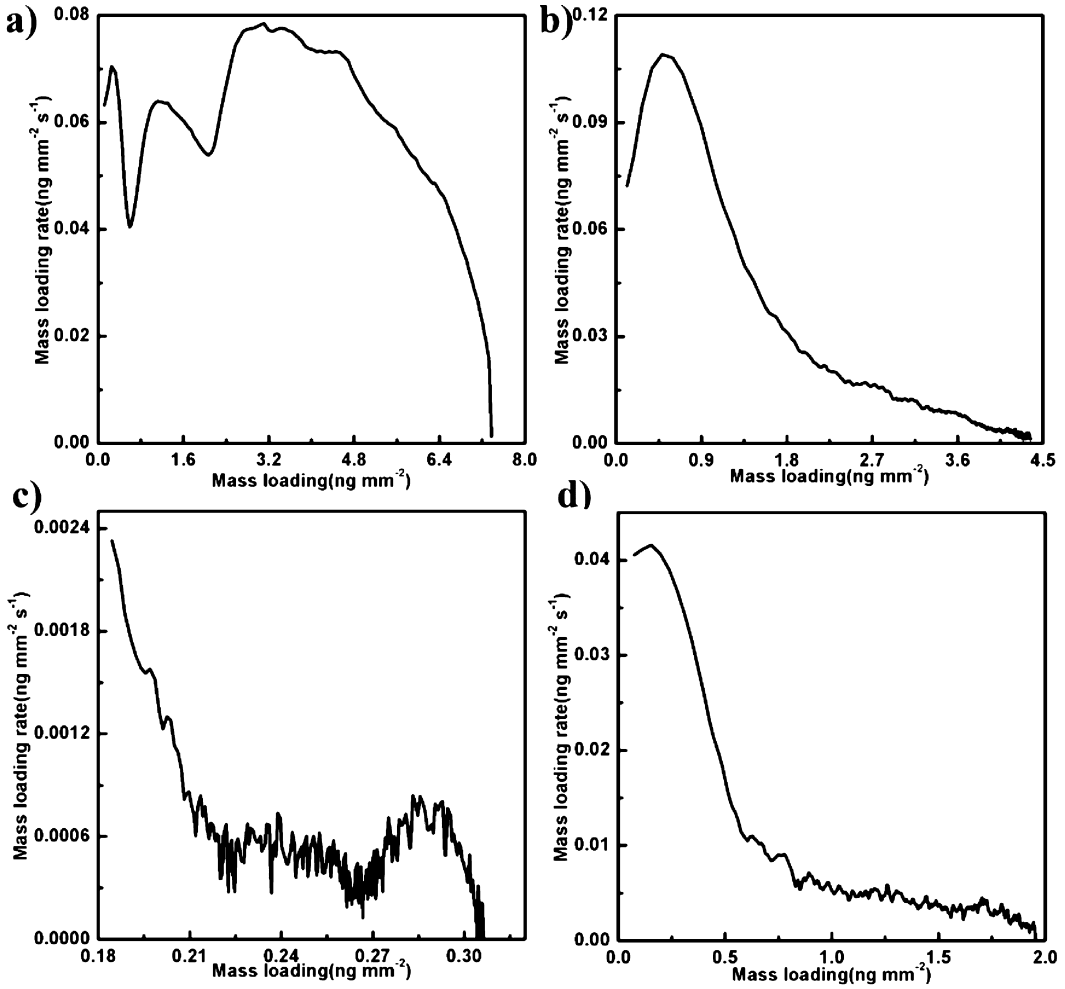

Figure 5. Changes in mass loading rate as a function of the mass loading of (a) DNA/Cu^{2+} and (b) DNA/$Co(NH_3)_6^{3+}$ complexes on the amino chip surface as well as (c) DNA/Ca^{2+} and (d) DNA/$Co(NH_3)_6^{3+}$ complexes on the silica chip surface during the initial adsorption stage.

It is hard for the DNA/Ca^{2+} complex to be adsorbed on the silica chip surface because of the negatively charged surface condition. Only 0.23 ng mm^{-2} complex was adsorbed on the silica chip surface, which is much lower than the amount of complex adsorbed on the amino chip surface. When the adsorption amount reached 0.27 ng mm^{-2}, the adsorbed layer structure changed and the following complex loosely attached on the surface similar to the adsorption of the DNA/Ca^{2+} complex on the amino chip surface. In contrast, the rearrangement of the adsorbed layer occurred only once, which happened twice in the adsorption on the amino chip surface. A relatively low surface coverage (0.27 ng mm^{-2}) can affect the following complex deposition pattern because of the strong electrostatic repulsion between the complex approaching the surface and the already adsorbed complex, as well as the weak interaction between the complex and silica surface. However, in the adsorption on the amino chip surface, the following complex deposition pattern can be affected by the already adsorbed complex layer only when the surface coverage reached 1.1 ng mm^{-2}.

The real-time mass, thickness, and density changes of the adsorption of the DNA/Cu^{2+} complex on the silica chip surface are shown in Figure 6. A relatively flat and dense layer formed rapidly on the surface at the beginning of the adsorption, and the layer density increased to the maximum. After this step, the thickness increased sharply and the density decreased

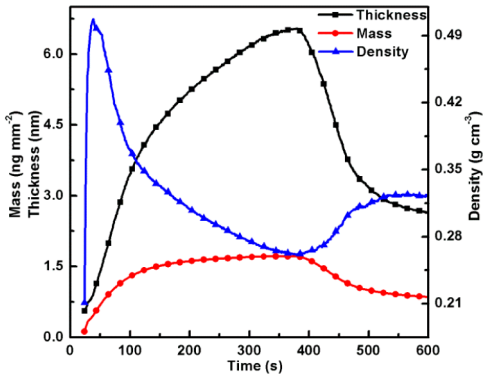

Figure 6. Real-time DPI measurements of thickness, mass, and density during the adsorption of the DNA/Cu^{2+} complex on the silicon chip surface.

dramatically, whereas the layer mass increased slightly. These changes in layer thickness, mass, and density demonstrate a deposition behavior change in the following adsorption process. Moreover, the mass loading rate curve (Figure 7) shows that the mass loading rate increased when the mass loading reached about 0.38 ng mm^{-2} (from this mass loading, the layer density began to decrease), indicating that the preadsorbed complexes

dx.doi.org/10.1021/am400813x | ACS Appl. Mater. Interfaces 2013, 5, 5025−5033

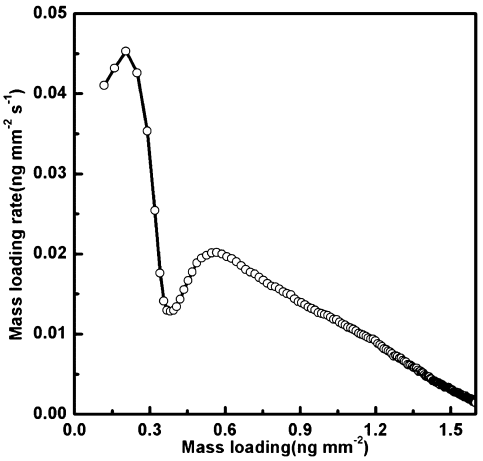

Figure 7. Changes in the mass loading rate as a function of the mass loading of the DNA/Cu^{2+} complex on the silica chip surface during the initial stage of adsorption from Figure 6.

rearranged themselves to enable the surface to take more complex from the aqueous solution.

The layer thickness change was also plotted against mass loading to determine how the preadsorbed complex affects the following complex deposition behavior (Figure 8). An

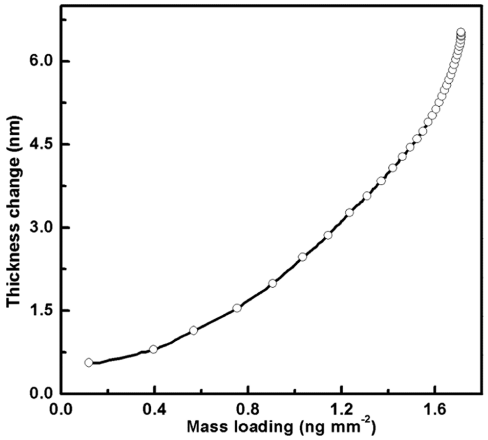

Figure 8. Changes in the layer thickness as a function of the mass loading of the DNA/Cu^{2+} complex on the silica chip surface during the initial stage of adsorption from Figure 6.

exponential curve was then obtained, which is different with the adsorption of the DNA/Cu^{2+} complex on the amino chip surface. The exponent-like curve indicates that the preadsorbed complex affects the deposition behavior of the approaching complex continuously, and so, the approaching complex can only attach more and more loosely on the surface during the adsorption process. This behavior is attributed to the strong electrostatic repulsion between the preadsorbed and approaching complexes as well as the relatively weak interaction between the complex and silica surface, resulting in the dramatic average layer thickness increase and sharp layer density decrease. After 6 min of adsorption, the valve switched and the surface was exposed to pure water. After rinsing, a sharp thickness decrease was observed, accompanied with a slight density increase and mass decrease. This is because that part of the loosely adsorbed complex was washed away.

In the adsorption of the DNA/$Co(NH_3)_6^{3+}$ complex on the amino or silica chip surface, the complex cannot cause the conformation rearrangement of preadsorbed complex because of the relatively weak repulsion between the complexes. Similar to the adsorption of the DNA/$Co(NH_3)_6^{3+}$ complex on the amino chip surface, no multiple mass loading rate increase was observed in the adsorption of the DNA/$Co(NH_3)_6^{3+}$ complex on the silica chip surface. Thus, only when the repulsion between DNA/cation complexes is strong enough that the approaching complex can induce the conformation rearrangement of the preadsorbed complex can the result be a multiple mass loading rate increase.

4. CONCLUSIONS

Three DNA/cation complexes with different charge conditions were prepared by simply dissolving DNA in 1 mM of $CaCl_2$, $CuSO_4$, and $Co(NH_3)_6Cl_3$ solutions. The zeta potentials and electrophoretic mobilities were measured using a Zetasizer Nano ZS instrument. The results show that the net negative charges of DNA/cation complexes decrease as follows: DNA/Ca^{2+} > DNA/Cu^{2+} > DNA/$Co(NH_3)_6^{3+}$. The adsorption process of these three complexes on amino and silica chip surfaces was evaluated in real time using DPI. A more compact complex layer formed on the amino chip surface under the same cation condition because of the relatively strong electrostatic interaction between the complex and amino chip surface. The most compact layer formed when the DNA/Ca^{2+} complex was adsorbed on the amino chip surface because of the strong electrostatic interaction with the amino chip surface. The DNA/$Co(NH_3)_6^{3+}$ complex can be adsorbed on the amino chip surface continuously, achieving the highest mass loading amount.

The mass, thickness, and density changes during adsorption were recorded in real time. The overall results show that all the adsorption processes exhibited multiphasic adsorption behavior because of the relatively strong electrostatic repulsion between the complexes or the geometric resistance. For the adsorption of DNA/Ca^{2+} and DNA/Cu^{2+} complexes on both amino and silica chip surfaces, the approaching complexes can induce the preadsorbed complexes to rearrange themselves to take more approaching complexes from solutions, resulting in the mass loading rate increase. Moreover, the crowded surface with preadsorbed complexes can affect the deposition pattern of the following complexes, which forced the approaching complexes to loosely attach on the surface.

During the adsorption of the DNA/$Co(NH_3)_6^{3+}$ complex on the amino and silica chip surfaces, no multiple mass loading increases were observed because of the weak electrostatic repulsion. Meanwhile, the preadsorbed complex can also induce the loose attachment of the following complex on the surface during the adsorption of the DNA/$Co(NH_3)_6^{3+}$ complex on the amino chip surface because of the geometric resistance. It is indicated that, only when the repulsion between complexes is strong enough, the approaching complex can result in the conformation rearrangement of the preadsorbed complex, while the preadsorbed complex can also induce the loose attachment of the approaching complex on the surface although the repulsion between complexes is weak when the surface is crowded. This study fully illustrates how the DNA/cation complex charge and how surface condition affect the DNA/cation complex adsorption behavior on the solid−liquid interface.

■ ASSOCIATED CONTENT

Supporting Information

The zeta potential distributions and electrophoretic mobility distributions of DNA/cation complexes; changes in layer thickness as a function of the mass loading of DNA/cation complexes on amino and silica chip surfaces. This material is available free of charge via the Internet at http://pubs.acs.org.

■ AUTHOR INFORMATION

Corresponding Author

*E-mail: hjliang@ustc.edu.cn. Fax: (+86) 551-63607824.

Notes

The authors declare no competing financial interest.

■ ACKNOWLEDGMENTS

This work was supported by the National Natural Science Foundation of China (20934004 and 91127046), NBRPC (2012CB821500 and 2010CB934500), and the "Bairen" fund of CAS.

■ REFERENCES

(1) Zhou, X. C.; Huang, L. Q.; Li, S. F. Y. *Biosens. Bioelectron.* **2001**, *16*, 85−95.
(2) Liss, M.; Petersen, B.; Wolf, H.; Prohaska, E. *Anal. Chem.* **2002**, *74*, 4488−4495.
(3) Pedano, M. L.; Rivas, G. A. *Biosens. Bioelectron.* **2003**, *18*, 269−277.
(4) Xiao, Y.; Lubin, A. A.; Heeger, A. J.; Plaxco, K. W. *Angew. Chem., Int. Ed.* **2005**, *44*, 5456−5459.
(5) Schena, M.; Shalon, D.; Davis, R. W.; Brown, P. O. *Science* **1995**, *270*, 467−470.
(6) Schena, M.; Shalon, D.; Heller, R.; Chai, A.; Brown, P. O.; Davis, R. W. *Proc. Natl. Acad. Sci. U.S.A.* **1996**, *93*, 10614−10619.
(7) Nelson, B. P.; Grimsrud, T. E.; Liles, M. R.; Goodman, R. M.; Corn, R. M. *Anal. Chem.* **2001**, *73*, 1−7.
(8) Kerman, K.; Ozkan, D.; Kara, P.; Meric, B.; Gooding, J. J.; Ozsoz, M. *Anal. Chim. Acta* **2002**, *462*, 39−47.
(9) Yang, A. Y.; Rawle, R. J.; Selassie, C. R. D.; Johal, M. S. *Biomacromolecules* **2008**, *9*, 3416−3421.
(10) Wang, J.; Xu, X. W.; Zhang, Z. X.; Yang, F.; Yang, X. R. *Anal. Chem.* **2009**, *81*, 4914−4921.
(11) Radu, D. R.; Lai, C. Y.; Jeftinija, K.; Rowe, E. W.; Jeftinija, S.; Lin, V. S. Y. *J. Am. Chem. Soc.* **2004**, *126*, 13216−13217.
(12) Torney, F.; Trewyn, B. G.; Lin, V. S. Y.; Wang, K. *Nat. Nanotechnol.* **2007**, *2*, 295−300.
(13) Xia, T. A.; Kovochich, M.; Liong, M.; Meng, H.; Kabehie, S.; George, S.; Zink, J. I.; Nel, A. E. *ACS Nano* **2009**, *3*, 3273−3286.
(14) Qin, F.; Zhou, Y. C.; Shi, J. L.; Zhang, Y. L. *J. Biomed. Mater. Res. A* **2009**, *90A*, 333−338.
(15) Boom, R.; Sol, C. J. A.; Salimans, M. M. M.; Jansen, C. L.; Wertheimvandillen, P. M. E.; Vandernoordaa, J. *J. Clin. Microbiol.* **1990**, *28*, 495−503.
(16) Berensmeier, S. *Appl. Microbiol. Biotechnol.* **2006**, *73*, 495−504.
(17) Manning, G. S. *Biophys. J.* **2006**, *91*, 3607−3616.
(18) Tan, Z. J.; Chen, S. J. *J. Chem. Phys.* **2005**, 122.
(19) Tan, Z. J.; Chen, S. J. *Biophys. J.* **2006**, *90*, 1175−1190.
(20) Song, Y. H.; Li, Z.; Liu, Z. G.; Wei, G.; Wang, L.; Sun, L. L. *Microsc. Res. Tech.* **2005**, *68*, 59−64.
(21) Todd, B. A.; Rau, D. C. *Nucleic Acids Res.* **2008**, *36*, 501−510.
(22) Allahyarov, E.; Lowen, H.; Gompper, G. *Phys. Rev. E* **2003**, 68.
(23) Besteman, K.; Van Eijk, K.; Lemay, S. G. *Nat. Phys.* **2007**, *3*, 641−644.
(24) Duguid, J.; Bloomfield, V. A.; Benevides, J.; Thomas, G. J. *Biophys. J.* **1993**, *65*, 1916−1928.
(25) Widom, J.; Baldwin, R. L. *Biopolymers* **1983**, *22*, 1595−1620.
(26) Bloomfield, V. A. *Biopolymers* **1997**, *44*, 269−282.
(27) He, S. Q.; Arscott, P. G.; Bloomfield, V. A. *Biopolymers* **2000**, *53*, 329−341.
(28) Ouameur, A. A.; Tajmir-Riahi, H. A. *J. Biol. Chem.* **2004**, *279*, 42041−42054.
(29) Conwell, C. C.; Hud, N. V. *Biochemistry* **2004**, *43*, 5380−5387.
(30) Bezanilla, M.; Manne, S.; Laney, D. E.; Lyubchenko, Y. L.; Hansma, H. G. *Langmuir* **1995**, *11*, 655−659.
(31) Pastre, D.; Pietrement, O.; Fusil, P.; Landousy, F.; Jeusset, J.; David, M. O.; Hamon, C.; Le Cam, E.; Zozime, A. *Biophys. J.* **2003**, *85*, 2507−2518.
(32) Pastre, D.; Hamon, L.; Landousy, F.; Sorel, I.; David, M. O.; Zozime, A.; Le Cam, E.; Pietrement, O. *Langmuir* **2006**, *22*, 6651−6660.
(33) Nguyen, T. H.; Elimelech, M. *Biomacromolecules* **2007**, *8*, 24−32.
(34) Nguyen, T. H.; Chen, K. L.; Elimelech, M. *Biomacromolecules* **2010**, *11*, 1225−1230.
(35) Nguyen, T. H.; Chen, K. L. *Environ. Sci. Technol.* **2007**, *41*, 5370−5375.
(36) Nguyen, T. H.; Elimelech, M. *Langmuir* **2007**, *23*, 3273−3279.
(37) Guzman, E.; Ortega, F.; Baghdadli, N.; Cazeneuve, C.; Luengo, G. S.; Rubio, R. G. *ACS Appl. Mater. Interfaces* **2011**, *3*, 3181−3188.
(38) Vandeventer, P. E.; Lin, J. S.; Zwang, T. J.; Nadim, A.; Johal, M. S.; Niemz, A. *J. Phys. Chem. B* **2012**, *116*, 5661−5670.
(39) Rawle, R. J.; Selassie, C. R. D.; Johal, M. S. *Langmuir* **2007**, *23*, 9563−9566.
(40) Su, X. D.; Wu, Y. J.; Knoll, W. *Biosens. Bioelectron.* **2005**, *21*, 719−726.
(41) Shumaker-Parry, J. S.; Campbell, C. T. *Anal. Chem.* **2004**, *76*, 907−917.
(42) Georgiadis, R.; Peterlinz, K. P.; Peterson, A. W. *J. Am. Chem. Soc.* **2000**, *122*, 3166−3173.
(43) Eskilsson, K.; Leal, C.; Lindman, B.; Miguel, M.; Nylander, T. *Langmuir* **2001**, *17*, 1666−1669.
(44) Cardenas, M.; Braem, A.; Nylander, T.; Lindman, B. *Langmuir* **2003**, *19*, 7712−7718.
(45) Cardenas, M.; Campos-Teran, J.; Nylander, T.; Lindman, B. *Langmuir* **2004**, *20*, 8597−8603.
(46) Nabok, A.; Tsargorodskaya, A.; Davis, F.; Higson, S. P. J. *Biosens. Bioelectron.* **2007**, *23*, 377−383.
(47) Zhao, X. B.; Pan, F.; Coffey, P.; Lu, J. R. *Langmuir* **2008**, *24*, 13556−13564.
(48) Guzman, E.; Ortega, F.; Baghdadli, N.; Luengo, G. S.; Rubio, R. G. *Colloids Surf., A* **2011**, *375*, 209−218.
(49) Lane, T. J.; Fletcher, W. R.; Gormally, M. V.; Johal, M. S. *Langmuir* **2008**, *24*, 10633−10636.
(50) Swann, M. J.; Peel, L. L.; Carrington, S.; Freeman, N. J. *Anal. Biochem.* **2004**, *329*, 190−198.
(51) Karim, K.; Taylor, J. D.; Cullen, D. C.; Swann, M. J.; Freeman, N. J. *Anal. Chem.* **2007**, *79*, 3023−3031.
(52) Mashaghi, A.; Swann, M.; Popplewell, J.; Textor, M.; Reimhult, E. *Anal. Chem.* **2008**, *80*, 3666−3676.
(53) Lillis, B.; Manning, M.; Berney, H.; Hurley, E.; Mathewson, A.; Sheehan, M. M. *Biosens. Bioelectron.* **2006**, *21*, 1459−1467.
(54) De Feijter, J. A.; Benjamins, J.; Veer, F. A. *Biopolymers* **1978**, *17*, 1759−1772.
(55) Tumolo, T.; Angnes, L.; Baptista, M. S. *Anal. Biochem.* **2004**, *333*, 273−279.
(56) Ikegami, A.; Imai, N. *J. Polym. Sci.* **1962**, *56*, 133−152.
(57) Delacruz, M. O.; Belloni, L.; Delsanti, M.; Dalbiez, J. P.; Spalla, O.; Drifford, M. *J. Chem. Phys.* **1995**, *103*, 5781−5791.
(58) Raspaud, E.; de la Cruz, M. O.; Sikorav, J. L.; Livolant, F. *Biophys. J.* **1998**, *74*, 381−393.
(59) Lee, D.; Gemici, Z.; Rubner, M. F.; Cohen, R. E. *Langmuir* **2007**, *23*, 8833−8837.
(60) Stumm, W.; Hohl, H.; Dalang, F. *Croat. Chem. Acta* **1976**, *48*, 491−504.
(61) Wu, Z. J.; Xiang, H.; Kim, T.; Chun, M. S.; Lee, K. *J. Colloid Interface Sci.* **2006**, *304*, 119−124.

(62) Briones, X. G.; Encinas, M. V.; Petri, D. F. S.; Pavez, J. E.; Tapia, R. A.; Yazdani-Pedram, M.; Urzua, M. D. *Langmuir* **2011**, *27*, 13524−13532.